Title

A Computational Model of Visual Pattern Discrimination in Toads

Permalink

Journal

Proceedings of the Annual Meeting of the Cognitive Science Society, 12(0)

Authors

Wang, DeLiang
Arbib, Michael A.

Publication Date

1990

Peer reviewed

A Computational Model of Visual Pattern Discrimination in Toads*

DeLiang Wang and Michael A. Arbib

Center for Neural Engineering, University of Southern California
Los Angeles, CA 90089-2520, U.S.A.

ABSTRACT

It has been found behaviorally that visual habituation in toads exhibits locus specificity and partial stimulus specificity. Dishabituation among different configurations of visual worm stimuli forms an ordered hierarchy. This paper presents a computational model of the toad visual system involved in pattern discrimination, including retina, tectum, and anterior thalamus. In the model we propose that the toad discriminates visual objects based on temporal responses, and anterior thalamus has differing representations of different stimulus configurations. This theory is developed through a large scale neural simulation. With a minimum number of hypotheses, we demonstrate that anterior thalamus in response to different worm stimuli shows the same hierarchy as shown in the behavioral experiment. The successful simulation allows us to provide an explanation of neural mechanisms for visual pattern discrimination. This theory predicts that retinal R2 cells play a primary role in the discrimination via tectal small pear cells (SP) while R3 cells refine the feature analysis by inhibition. The simulation also demonstrates that the retinal response to the trailing edge of a stimulus is as crucial for pattern discrimination as to the leading edge. New dishabituation hierarchies are predicted by shrinking stimulus size and reversing stimulus-background contrast.

1. Introduction

After repeated presentation of the same prey dummy in their visual field, toads and frogs may reduce the number of orienting responses toward the moving stimulus. This phenomenon is called *habituation*. Habituation has been extensively investigated, ranging from invertebrates, like *Aplysia* [1], where habituation seems to be independent of the specific patterning of the stimulus, to mammals where habituation exhibits stimulus specificity so that habituation to a certain stimulus pattern may be dishibituated by a different stimulus pattern [2]. Visual habituation in toads has the following characteristics [3]:

(1) *Locus specificity*. After habituation of an orienting response to a certain stimulus applied at a given location, the response can be released by the same stimulus applied at a different retinal locus.

(2) *Partial stimulus specificity*. Another stimulus given at the same locus may restore the response habituated by a previous stimulus. Only certain stimuli can dishabituate a previously habituated response. Experimental results [4] show that this dishabituation relation forms an ordered hierarchy of stimulus patterns (Figure 1), where only a pattern at a higher level can dishabituate the habituated responses of the stimuli at lower levels. We call this kind of stimulus specificity *partial* because the dishabituation relation is ordered rather than mutual.

The biological relevance of the stimulus-specific habituation phenomena may be to keep the IRM (innate releasing mechanism) for prey catching alert to "new" stimuli. However, the dishabituation hierarchy suggests that it is *configurational cues* of the stimulus and not only its "newness" which decide the toad's response [4]. It is reasonable to assume that toads have not developed the advanced spatial shape recognition capability of higher animals, but have developed the ability to recognize certain stimulus configurations, which, for example, are used in discriminating prey and predator.

Although Ewert and Kehl [4] demonstrated the behavioral responses leading to the hierarchy, they did not investigate the neural mechanisms involved, which must involve visual centers such as retina and tectum. For toads to exhibit the dishabituation hierarchy, there have to be differing representations of different stimulus shapes somewhere in their visual system. Unfortunately, physiological studies provide very little data on the response of these centers to a variety of stimulus shapes (for a review see [5]). In the Lara-Arbib model for this stimulus-specific habituation behavior [6], the discrimination of the stimuli in Fig.1 is made by retinal ganglion cell R2. They introduce a group of *ad hoc* functions each of which is used to emulate how a specific stimulus traverses the

---

excitatory receptive field (ERF) of R2, but they did not give any biological justification for that *ad hoc* group of functions.

We develop a model for discriminating different worm-like stimuli which is able to demonstrate a class of cells whose firing rate in response to the different stimulus types exhibits the same order as shown in the dishabituation hierarchy. We hypothesize that these cells lie in the anterior thalamus, and thus suggest new physiological experiments to test our theory.

2. Distributed vs. Temporal: Basic Hypothesis

An object can be naturally coded by distributed activity in a group of neurons, or at some high level by firing activities of single cells. Here the former is denoted as *distributed coding* and the latter as *temporal coding*. Distributed coding is strongly favored by theoreticians due to considerations of reliability, although it seems that both are used in the object representation of primates. Do anurans represent various worm-like stimuli by distributed coding or temporal coding? Our basic hypothesis is that anurans represent objects by *temporal coding*. More specifically, the firing rate of neurons in some neural center of the toad visual system is higher in response to a stimulus in the upper part of the hierarchy than one in the lower part.

Generally speaking, distributed representation corresponds to neural associative memory, where the difference between two patterns is measured by their Hamming distance. However, the distributed coding fails to explain the partial stimulus-specificity since no ordering can be embodied in associative memory. This might be the case in higher animals like mammals where dishabituation could be accounted for by a comparator model [2], but this contradicts the observed ordered hierarchy in toads [4]. Moreover, the discrimination capability of toads is rather limited. In their original experiment, Ewert and Kehl did not find shapes other than those in Fig.1 that could be discriminated (Ewert, personal communication 1989). This limitation seems straightforward based on our hypothesis because the frequency spectrum can only be markedly differentiated into a number of levels and therefore the capacity is severely limited compared to distributed coding. It could be that amphibians, a phylogenetically older species than mammals, have not yet achieved the advanced distributed coding which has immense potentials in terms of capacity. Looked from the other direction, however, amphibians do reach the partial stimulus-specificity which does not seem to be obtained in invertebrates [1].
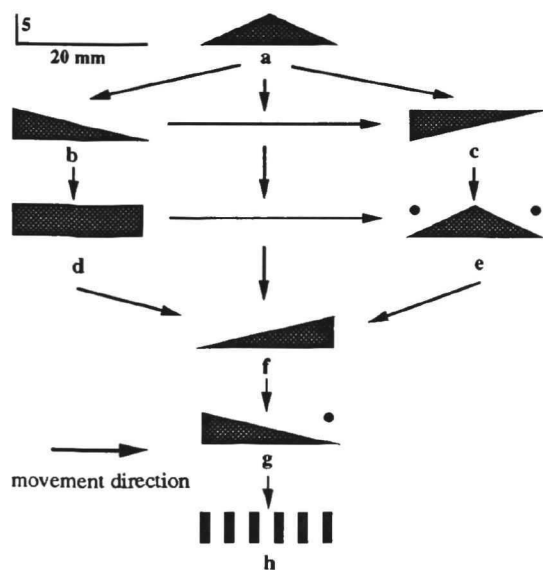

Figure 1. Dishabituation hierarchy for worm stimuli used in stimulus-specific habituation of toads. One stimulus can dishabituate all the stimuli below it. On the same level the left stimulus can slightly dishabituate the right one (from [4]).

A major criticism of temporal representation is that the reliability of this coding paradigm depends on single cells which are vulnerable in the nervous system. However, this criticism can be answered through redundancy of a cell population, as is actually the case in the nervous system. Neighboring neurons have almost the same receptive field, so the malfunction of a few cells would not matter so much because their neighbors could easily replace their role. If a localized neuron population is destroyed, we should expect localized malfunction of the temporal representation. In the anuran visual system, a localized scotoma from a localized lesion is found in various visual centers starting from retina. This suggests that visual information is represented in anurans by a temporal paradigm, since in classic models of distributed coding (for example see [7]) localized cell loss seems impairing only general associative abilities.

A direct prediction of our basic hypothesis is that the ordered dishabituation hierarchy is underlain by the different firing rates of certain neurons in the toad visual system. This prediction will be tested in simulations presented in the following sections. In the experiment of Ewert and Kehl [4], all stimuli are $20mm$ long and $5mm$ high. With a $70mm$ distance of presentation from the toads, each stimulus is about $16°$ long and $4°$ high. The dot used is $1\,mm$ in diameter which is about $1°$.

The locus specificity that toads and frogs show for dishabituation conforms well to temporal coding. *Retinotopy*, one form of locus specificity, has been extensively observed both in tectum and in thalamus of toads [3]. Although the adaptive significance for anurans treating the same stimulus at different locations as different ones

is not finally resolved, it does demand extra memory capacity compared to a memory scheme which achieves locus-constancy, but toads need an accurate location memory.

3. Retinal Coding

An elementary model of the retinal receptive field uses two mechanisms in deciding retinal responses: (1) an excitatory center and (2) an inhibitory surround. Both mechanisms are described by spatially Gaussian-distributed curves around a common midpoint, and the whole neuronal response is formed as a difference of Gaussians (DOG). Our retinal analysis is mainly based on the Teeters' retina model [8] since it provides the most detailed account of the toad retina to date. The model for the anuran retina prior to ganglion cells consists of four cascade layers: *receptor*, *horizental*, *biopolar* and *amacrine*. Three different types of ganglion cell were identified in the retinotectal projection of toads which correspond to R2, R3 and R4 in frogs. The response of R2 and R3 to three classes of stimuli used in the Ewert laboratory is summarized in Fig.2 [9]. Note that only the response to the leading edge is shown in the recording. In the model, each cell type corresponds to a two dimensional matrix, with a single cell identified by $m(i,j,t)$ representing the membrane potential of the neuron at position (i, j) at time t. $I(i,j,t)$, the input to the neuron at position (i, j), is created by a convolution of a kernel which approximates a DOG with the corresponding output from a previous cell matrix

$$I(i,j,t) = (k*S)(i,j,t) \tag{1}$$

where $*$ represents convolution, S indicates the output of the previous layer, and a kernel element $k(x,y)$ is defined as

$$k(x,y) = \begin{cases} W_e \, exp[-(x^2+y^2)/(2\sigma_e^2)] - W_i \, exp[-(x^2+y^2)/(2\sigma_i^2)] & if \ x^2+y^2 \leq R^2 \\ 0 & otherwise \end{cases} \tag{2}$$

where R is the radius of a receptive field measured in degrees of visual angle, W_e and W_i combine together to determine the weight from the previous layer to the current one. The Mexican hat of the kernel, the activity distribution of a receptive field, is uniquely determined by parameters W_e, W_i, σ_e, and σ_i.
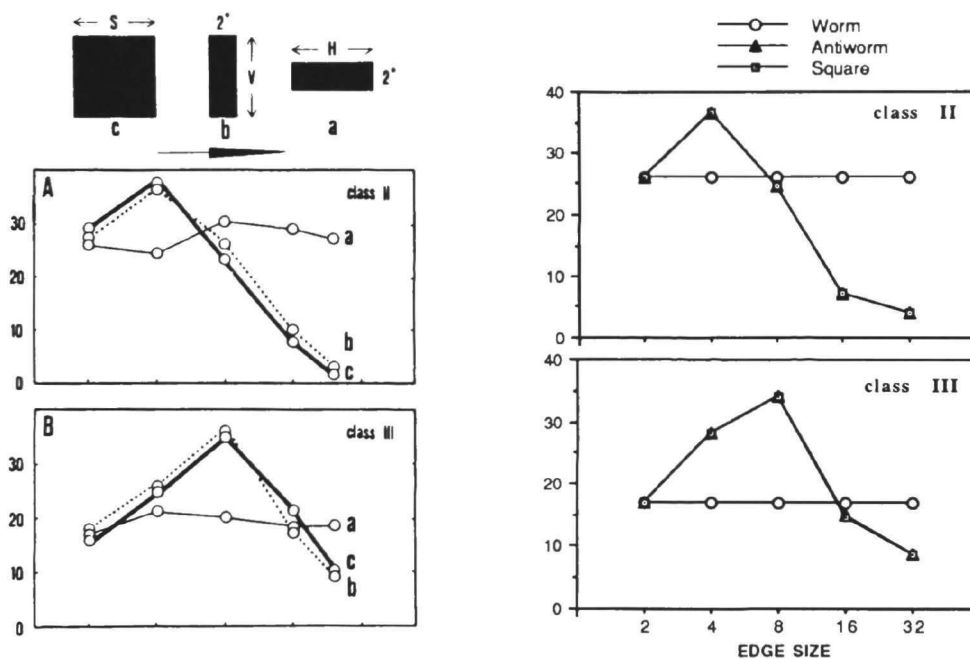

Figure 2. The model response of R2 and R3 to worm, antiworm, and square. left: the experimental data [9]. right: Response of our modified retina model. Each point in the figure represents the temporal average firing rate in response to the corresponding stimulus.

600

The retina model in this paper is a modified version of the Teeters model which more closely simulates the biological data. Simulation results from our modified model are presented in Fig.2 for the two types of ganglion cells respectively, together with the biological data. The average firing rate of a neuron is computed by the temporal integration of its instantaneous firing rate divided by the time period during which a non-zero firing rate is consecutively elicited. The response of R4 is neglected due to its insensitivity to difference between the worm stimuli. Our simulation result has demonstrated that without a significant trailing edge response, it is impossible to discriminate the different worm configurations even at the retina level.
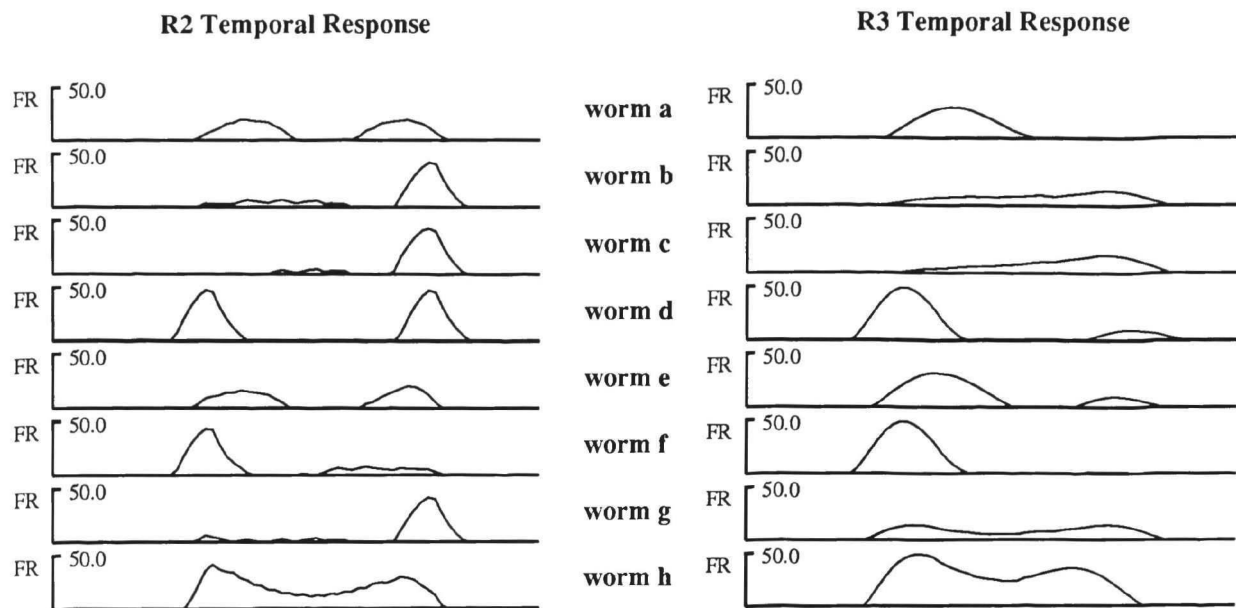
R2 Temporal Response   R3 Temporal Response

Figure 3. The temporal firing rate of R2 (**left**) and R3 (**right**) to the *8* worm-like stimuli from the retina model. Time runs from left to right, and all the stimuli are moving from left to right. The unit of the numbers in the figure is impulses per second.

Tsai and Ewert [10] recently found that R2 cells show no preference in response to both edges of a stimulus if neuronal adaptation is not taken into account, while R3 cells show a much stronger off-channel (from white to black) than on-channel (from black to white) response, which correlates with the behavior. In this simulation, the R3 response to trailing edge is modeled with a *1.0/0.2*, and the R2 response with a *1.0/1.0* ratio of off- to on-channel contribution. In particular, the R2 membrane potential is described by

$$\tau_{r2} \frac{dm_{r2}(i,j,t)}{dt} = -m_{r2}(i,j,t) + (k_{r2} * (S_{ath} + S_{atd}))(i,j,t) \tag{3}$$

where τ is the time constant of the above leaky integrator model. Subscripts indicate the neuron types, e.g., k_{r2} stands for the kernel of a R2 cell as defined in (2). The detailed definition of S_{ath} and S_{atd} is given in [8].

Fig.3 shows the temporal responses of a R2 neuron and a R3 neuron to the 8 worm-like stimuli in Fig.1 from our modified retina model. Here only firing rate is displayed, which equals $m(t)$ if $m(t) > 0$ and 0 otherwise for both R2 and R3 cells. In terms of single cell response, a vertical bar of *4°* height elicits the strongest response in both R2 and R3 cells, and the more inclined is a stimulus edge, the less efficient is it to trigger a retinal response. This is because the more inclined is a stimulus edge with the same vertical height, the larger does it encroach on the inhibitory surround and longer is the duration of the response. Note the R2 effect of the dots in worm **e** relative to **a** and worm **g** relative to **b** in Fig.3. Since the dot is encroaching R2's IRF while the edges of stimuli **e** and **g** traverse R2's ERF, worms **e** and **g** elicit smaller R2 responses than worms **a** and **b** respectively. Note also that the distance between the two peaks for R2 leading/trailing response corresponds to the distance between the middle points of the leading edge and the trailing edge of the stimulus. In the simulation, the density of receptors is *1 cell / 0.5 degree* while the ganglion cell density is *1 cell / 2 degree* resulting in a *4 to 1* density ratio. Each ganglion cell has a receptive field of approximately *20x20* degrees or *40x40* receptors.

4. Tectal Relay

Based on anatomical data and functional lesion data, Ewert [11] suggested that the basic pathway for habituation is: *retina → tectum → aTH* (anterior thalamus) *→ MP* (medial pallium) *→ tectum*. This pathway is refered to as *loop(2)* and is generally supposed to be responsible for modulation of the innate releasing behaviors of amphibians. In this paper, we are only concerned with the first part of this loop: *retina → tectum → aTH*, where the discrimination of the stimuli is presumably achieved.

In this model, the optic tectum discriminates prey from predator, but we hypothesize that it does not play a major role in the finer pattern discrimination that underlies the dishabituation hierarchy, but rather relays the input from retina to anterior thalamus where the visual information is further processed and carried up to telencephalon. As for stimulus-specific habituation, behavioral data show that the releasing values for all the stimuli in the hierarchy are almost the same [4]. Also, the prey-catching behavior shows off-channel preference, which correlates very well with the neuronal activities in R3 and T5(2) cells. This finding leads Tsai and Ewert [10] to propose that R3, not R2, carries the primary information to the prey analysis circuitry located in tectum. However, as pointed out in the previous section, the response to the trailing edge should have a significant role in worm discrimination. This suggests that R2, so called "net convexity detectors", may be more involved in the discrimination of worm-like stimuli than R3. This trailing edge consideration tends to downplay the tectum as a major neural center on "subworm" discrimination.

Lázár et.al. [12] found that in anurans the main projection units to the anterior diencephalon from tectum are the small piriform neurons (SP), which are located in layer 8 of the tectum. This important finding leads us to assume that SP cells relay the visual information concerning worm discrimination. In the present model SP cells receive R2 inputs, which is consistent with the tectum model of Cervantes et al. [13], and projects to anterior thalamus. Since R2 projects to SP topographically and the SP's role in this model is to relay R2 activity, to simplify the implementation the neuronal response of SP is made equal to that of R2 to the worm stimuli.

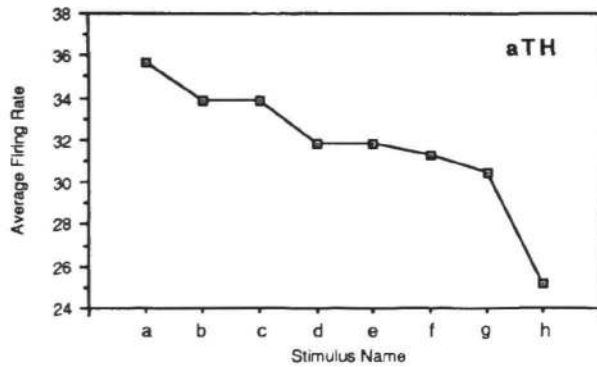## 5. Integration in Anterior Thalamus

Figure 4. AT response to the 8 worm-like stimuli shown in Figure 1. The 8 average firing rates are ordered, which corresponds to the ordered hierarchy in Figure 1. In the simulation, $\tau_{at} = 0.065$, $\theta_{at} = 13.0$, $W_{sp}^e = 0.0091$, $W_{sp}^i = -0.003$, $W_{r3}^e = 0.0095$, $W_{r3}^e = -0.003$, $m_1 = n_1 = 6$, and $m_2 = n_2 = 12$.

The anterior thalamus receives ascending R3 retinal projections [5] and SP tectal projections [12]. Among other ascending projections to telencephalon, aTH has a direct projection to the medial pallium, where visual information is presumably stored. Compared to the optic tectum and the caudal thalamus, aTH is much less understood in terms of neurophysiology and morphology. Functionally, it has been suggested that aTH forms part of the anatomical substrate by which visual information reaches the medial pallium [14], and it was found that large ablations of aTH usually depressed the prey-catching behavior [15]. Also aTH has been proposed as part of the modulatory loop(2) [11]. However, the kind of visual processing performed by aTH remains unknown.

We offer in the present model a definite hypothesis: Based on the special position of aTH and our previous analysis of visual information processing, we propose that it is the anterior thalamus where the pattern discrimination is finally achieved by neuronal responses. In this model, AT neurons receive excitatory-center inhibitory-surround inputs from tectal SP cells, and direct inhibitory inputs from R3 cells. Quantitatively,

$$\tau_{at} \frac{dm_{at}(i,j,t)}{dt} = -m_{at}(i,j,t) + (k_{at1}*S_{sp})(i,j,t) - Max\,[0, (k_{at2}*S_{r3})(i,j,t)] \tag{4}$$

where $k_{at1}(x,y) = W_{sp}^e$, if $|x| \leq m_1$ and $|y| \leq m_1$; W_{sp}^i, if $m_1 < |x| \leq m_2$ and $m_1 < |y| \leq m_2$; and 0 otherwise. $k_{at2}(x,y) = W_{r3}^e$, if $|x| \leq n_1$ and $|y| \leq n_1$; W_{r3}^i, if $n_1 < |x| \leq n_2$ and $n_1 < |y| \leq n_2$; and 0 otherwise. $S_x(t)$, $x \in \{sp, r3\}$, represents the firing rate of neuron type x, and $S_{at}(t) = m_{at}(t) - \theta_{at}$, if $m(t) \geq \theta_{at}$ and 0 otherwise.

602

Receptor Layer

BD layer

BH layer

ATD layer

ATH layer

R2 layer

R3 layer

R4 layer

SP layer

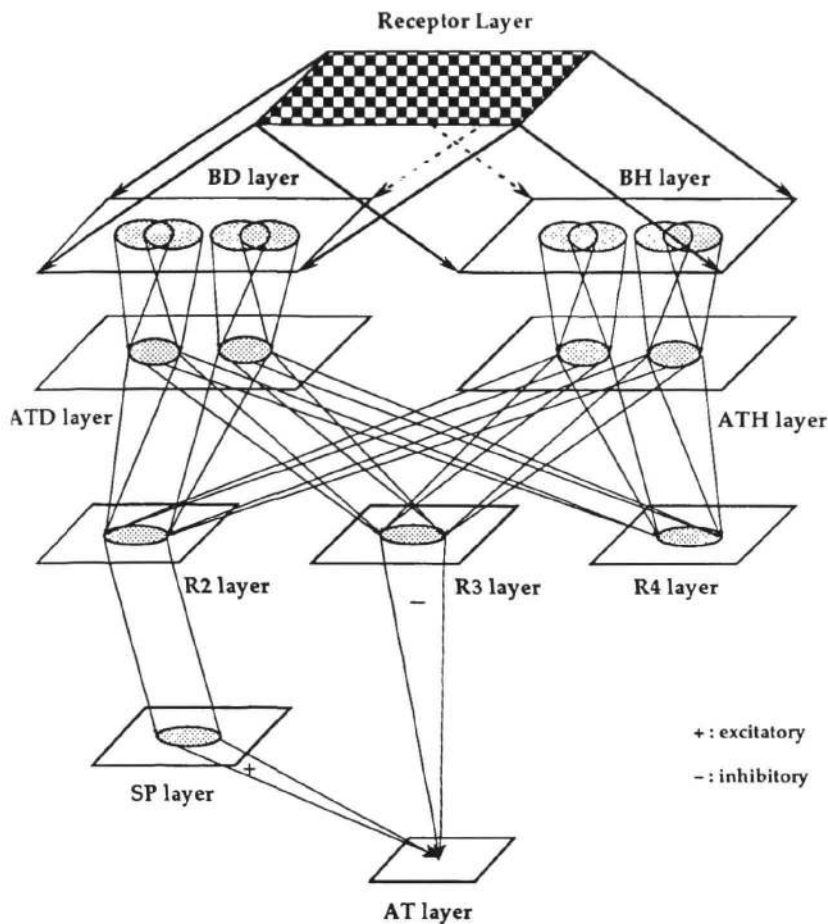+ : excitatory

− : inhibitory

AT layer

Figure 5. Diagram of the entire model used in this simulation project. Retina, tectum and anterior thalamus have been incorporated in the model. For explanation see text.

Figure 4 shows the average firing rates of a single AT neuron to the 8 worm-like stimuli. See the legend for the values of the parameters introduced above. The result clearly matches the ordered dishabituation hierarchy in Fig.1. Not only do stimuli higher in the hierarchy generate larger AT responses, but the stimulus pairs b–c and d–e which are on the same level in the hierarchy generate nearly equal responses. The modeled dishabituation hierarchy is the same as in Fig.1 except that the model cannot create the preference of stimulus b over c, which is weakly exhibited in the animal.

In summary, we propose the following mechanisms to explain the dishabituation hierarchy in Fig.1.

(1) Both the leading edge and the trailing edge of a worm stimulus have to be taken into consideration.

(2) The receptive field of AT neurons is big enough to "see" both the leading and the trailing edge. Stimulus a elicits the biggest response, particularly bigger than stimulus d, because both diagonal edges elicit strong responses in R2 cells (see Fig.3) and these responses can be best integrated in AT cells due to the small distance between the midpoints of its leading and trailing edge response.

(3) Stimuli b and c are prefered to stimulus f because the inhibition of R3 cells, which has off-channel preference, is bigger for f than for b and c.

(4) Stimuli with dots appear lower in the hierarchy because they elicit smaller R2 response due to IRF interaction.

(5) A striped pattern elicits the smallest response in AT neurons because of R3 inhibition.

6. Conclusion and Predictions

Inspired by the behavioral results [4] resulting in the dishabituation hierarchy, the present model represents an integration of behavioral, physiological, anatomical, and theoretical studies on the brain in order to postulate mechanisms for pattern discrimination in amphibians.The model is tested by a large-scale computer simulation which incorporates retina, tectum and anterior thalamus. The anatomy of the model is summarized in Fig.5. In the figure, conical projections represent on-center off-surround convergence, while the cylindrical projection from the R2 layer to the SP layer represents a 1 to 1 mapping. The connections from the receptor layer to both the BD and BH layer also constitute a small many-to-one convergence. The receptor layer contains *140x140* cells which correpond to *70˚x70˚* visual field. Bipolar and amacrine cell layers consist of *140x140* cells respectively which correspond to the receptor layer. Three types of ganglion cells have been modeled, each consisting of *25x25* cells which correspond to *70˚x70˚* visual field since the ganglion cells have *20˚* RF and lie *2˚* apart. The R2 layer projects to the SP layer in the tectum, and the SP layer and R3 layer together converge on the AT layer in the anterior thalamus, where the
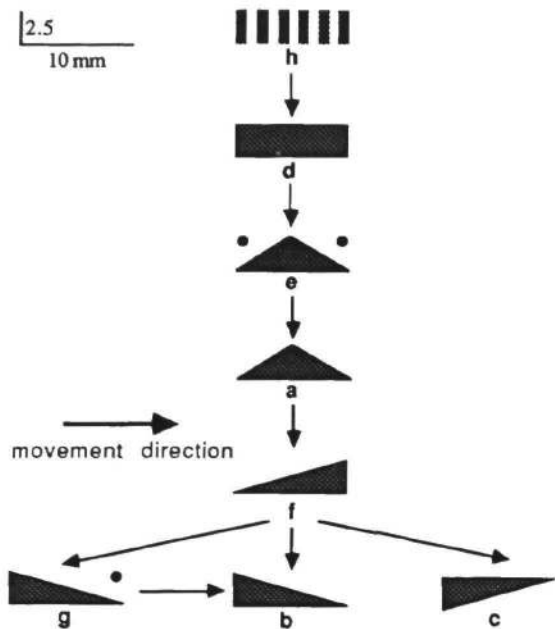
Figure 6. Dishabituation hierarchy predicted from this model by shrinking stimulus size. All the stimuli are *10 mm* long and *2.5 mm* high. The same set of stimulus configurations is used as in Figure 1.
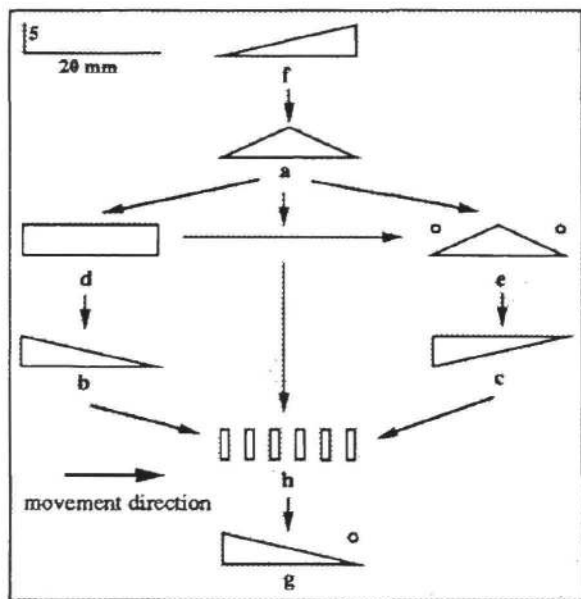

Figure 7. Dishabituation hierarchy predicted from this model by reversing contrast direction. In contrast to Fig.1, white stimulus is moving against black background. The same set of stimulus configurations is used as in Figure 1.

worm-like pattern discrimination is finally achieved. The entire simulation contains about *100,000* cells. Bitmap stimuli are used.

The simulation of the pattern discrimination was done after the retina model was fixed. Since the retinal responses are constrained strongly by the experimental data [9, 10], the retinal model, even its various parameters, cannot be modified to fit other simulation purposes since otherwise the original match between the model and the data could not be preserved. This represents a real challenge for later simulations based on retinal output. On the other hand, this requirement also provides a strict testbed for hypotheses and neural models.

A major postulate of this paper is that toads represent objects by temporal coding. This theory explains the locus-specificity of habituation and the dishabituation hierarchy in the following way: a stimulus at a higher position of the hierarchy elicits a stronger response at some location than that elicited by a stimulus at a lower position. Based on the theory, we have proposed a concrete neural model which successfully simulates the experimental data. The following list provides a number of model predictions:

(1) When the animal is presented with the different worm-like stimuli, they will elicit different neuronal responses at a certain neural center, and the order exhibited based on average firing rate corresponds to the order exhibited in the dishabituation hierarchy.

(2) Retinal ganglion cell type R2 plays a primary role in the discrimination of the stimuli, since R2 responds best to small moving objects and detects equally well both the leading and trailing edge of a stimulus.

(3) In the discrimination of different "sub-worms", the optic tectum serves only to relay information from retina to aTH via SP cells.

(4) R3 cells have an inhibitory role in worm pattern discrimination. This is due to their off-channel preference (from white to black).

(5) Anterior thalamus is the structure which reflects the final pattern discrimination. This structure receives excitatory projections from SP and inhibitory projections from R3.

In terms of stimulus size, the current model will create different hierarchies based on different sizes of worm-like stimuli. After completing the previous simulations, we shrinked the size of all the stimuli to *10mm* long and *2.5mm* high correponding to *8°* by *2°*, and tested these stimuli. Fig.6 shows the dishabituation hierarchy predicted by this model. A remarkable difference has been revealed compared to Fig.1. Particularly, stimulus **h** lies at the top, in contrast to the bottom position in Fig.1, and stimuli with dots appear higher in the hierarchy, reversing the original relation exhibited in Figure 1. Our

explanation is that since the stimulus size is halfed compared to Fig.1, the previous IRF interaction in the R2 receptive field are converted into an ERF interaction which strengthens overall responses. This ERF interaction is particularly manifested by stimulus **h**. Note that the R3 inhibition in AT neurons is relatively smaller than the excitation from SP cells, and thus cannot prevent stimulus **h** from inducing a strong AT response. This model discovery leads us to postulate that the effect of dot and striped pattern is relative to stimulus size in pattern discrimination. Furthermore in terms of multiple stimulus effect, this prediction suggests that if multiple stimuli lie close to each other they tend to cooperate to form a stronger response than any one of them, otherwise if the stimuli lie far from each other they tend to compete and conteract each other's response.

In this model of pattern discrimination both on-channel and off-channel effects are considered important. We have tested the same stimulus patterns as in Fig.1 but reversed the contrast-direction, i.e. white stimuli moving against a black background (w/b). A new dishabituation hierarchy is found in our simulation, as shown in Figure 7. The response of R2 cells with w/b is the same as with b/w, but now R3 cells show a trailing edge preference. These predictions have to be tested experimentally.

References

[1] Kandel E. (1976): *Cellular basis of behavior: an introduction to behavioral neurobiology.* Freeman: New York.

[2] Sokolov E. (1975): Neuronal mechanisms of the orienting reflex. In: *Neuronal mechanisms of the orienting reflex.* Sokolov E. and Vinogradova O. (eds), Lawrence Erlbaum/Hillsdale: New York.

[3] Ewert J.P. (1984): Tectal mechanisms that underlie prey-catching and avoidance behaviors in toads. In: *Comparative Neurology of the Optic Tectum,* Vanegas H. (ed). Plenum: New York, London.

[4] Ewert J.P. and Kehl W. (1978): Configurational prey-selection by individual experience in the toad *Bufo bufo. J.Comp.Physiol.* 126, 105-114.

[5] Grüsser O.J. and Grüsser-Cornehls U. (1976): Neurophysiology of the anuran visual system. In: *Frog Neurobiology.* Llinas R. and Precht W. (eds). Springer: Berlin, Heidelberg, New York.

[6] Lara R. and Arbib M.A. (1985): A model of the neural mechanisms responsible for pattern recognition and stimulus specific habituation in toads. *Biol.Cybern.* 51, 223-237.

[7] Hopfield J.J. (1982): Neural networks and physical systems with emergent collective computational abilities. *Proc.Nalt.Acad.Sci. USA* 79, 2554-2558.

[8] Teeters J.L. (1989): A simulation system for neural networks and model for the anuran retina. *Technical Report* 89-01, Center for Neural Engineering, University of Southern California, Los Angeles.

[9] Ewert J.P. (1976): The visual system of the toad: behavioral and physiological studies on a pattern recognition system. In: *The amphibian visual system: a multidisciplinary approach,* Fite K. (ed). Academic Press: New York.

[10] Tsai H.J. and Ewert J.P. (1987): Edge preference of retinal and tectal neurons in common toads (*Bufo bufo*) in response to worm-like moving stripes: the question of behaviorally relevant "position indicators". *J.Comp.Physiol.* A, 161, 295-304.

[11] Ewert J.P. (1986): Neuroethology: toward a functional analysis of stimulus-response mediating and modulating neural circuitries. In *Cognitive processes and spatial orientation in animal and man,* part 1, Ellen P. and Thinus-Blonc C. (eds). Dordrecht: Martinus Nijhoff.

[12] Lázár Gy., Toth P., Csink Gy., and Kicliter E. (1983): Morphology and location of tectal projection neuron in frogs: A study with HRP and Cobalt-filling. *J.Comp.Neurol.* 215, 108-120.

[13] Cervantes-Perez F., Lara R., and Arbib M.A. (1985): A neural model of interactions subserving prey-predator discrimination and size preference in anuran amphibians. *J.theor.Biol.,* 113, 117-152.

[14] Neary T.J. and Northcutt R. (1983): Nuclear organization of the bullfrog diencephalon. *J.Comp.Neurol.,* 213, 262-278.

[15] Ingle, D. (1980): The frog's detection of stationary objects following lesions of the pretectum. *Behav.Brain Res.,* 1, 139-163.